Inorg. Chem. **2009**, *48*, 2873−2879

A Polynuclear $d^{10}-d^{10}$ Metal Complex with Unusual Near-Infrared Luminescence and High Thermal Stability

Chengyang Yue,[†,‡] Chunfeng Yan,[†] Rui Feng,[†] Mingyan Wu,[†] Lian Chen,[†] Feilong Jiang,*[,†] and Maochun Hong*[,†]

Fujian Institute of Research on the Structure of Matter, Chinese Academy of Sciences, Fuzhou, Fujian 350002, China, and Department of Chemistry, Jining University, Qufu, Shandong 273155, China

Received September 30, 2008

Three $d^{10}-d^{10}$ transition-metal complexes with organosulfur ligands, $Cu_6(btt)_6$ (**1**), $Cu_4(btt)_4$ (**2**), and $Ag_6(bmt)_6 \cdot 6THF$ (**3**) (Hbtt = 2-benzothiazolethiol, Hbmt = 2-benzimidazolethiol, and THF = tetrahydrofuran), were synthesized and characterized. Complexes **1** and **2** with similar coordination environments are isomers crystallized from the same solvothermal reactions, but they cause great differences in both the structures and luminescent behaviors. The hexanuclear cluster **1** exhibits unusual near-infrared luminescence and high thermal stability, while complex **2** with tetranuclear cores and stronger metal−metal bonds shows an intense red emission like that from complex **3**.

Introduction

Luminescent transition-metal complexes are currently under investigation for both theoretical and applicative purposes because of their capability to exhibit metal···metal interactions, which have important influence on their spectroscopic behaviors and emission energies.[1] Among these studies, investigations about near-infrared (NIR) materials, particularly in the 700−900 nm region, remain relatively sparse. It is reported that such NIR materials have been sought for biological, diagnostic, and therapeutic applications because cells, tissues, and other biological molecules exhibit little autofluorescence in this region.[2]

In the research of luminescent complexes over decades,[3] functional materials containing Cu^I and Ag^I ions with d^{10} closed-shell electronic configurations have attracted much attention considering their abundant resources, low cost, and nontoxic properties compared to noble metal complexes, e.g., Re^I,[4] Os^{II},[5] Ir^{III},[6] Rh^I,[7] Pt^{II}, and Au^I.[8] These obvious advantages lend Cu^I and Ag^I complexes as excellent candidates of luminescent materials with the potential toward mass production and broad application. Furthermore, organosulfur ligands are frequently applied as bridging ligands for adjacent transition-metal sites in the design of luminescent materials

* To whom correspondence should be addressed. E-mail: fjiang@fjirsm.ac.cn (F.J.), hmc@fjirsm.ac.cn (M.H.). Tel: +86-59-83792460. Fax: +86-59 -3714946.

† Chinese Academy of Sciences.

‡ Jining University.

(1) (a) Shi, L. L.; Liao, Y.; Zhao, L.; Su, Z. M.; Kan, Y. H.; Yang, G. C.; Yang, S. *J. Organomet. Chem.* **2007**, *692*, 5368–5374. (b) Ding, Y.; Chen, H. L.; Wang, E. B.; Xu, X. X.; Wang, X. L.; Qin, C. *Transition Met. Chem.* **2008**, *33*, 183–187. (c) Jimenez-Pulido, S. B.; Linares-Ordonez, F. M.; Moreno-Carretero, M. N.; Quiros-Olozabal, M. *Inorg. Chem.* **2008**, *47*, 1096–1106. (d) Lin, J. G.; Su, Y.; Tian, Z. F.; Qiu, L.; Wen, L. L.; Lu, Z. D.; Li, Y. Z.; Meng, Q. J. *Cryst. Growth Des.* **2007**, *7*, 2526–2534. (e) Hu, X. Y.; Liu, X. J.; Feng, J. K. *Chin. J. Chem.* **2007**, *25*, 1370–1378.

(2) (a) Aubin, J. E. *J. Histochem. Cytochem.* **1978**, *17*, 36. (b) Werts, M. H. V.; Woudenberg, R. H.; Emmerink, P. G.; van Gassel, R.; Hofstraat, J. W.; Verhoeven, J. W. *Angew. Chem., Int. Ed.* **2000**, *39*, 4542. (c) Licha, K. *Top. Curr. Chem.* **2002**, *222*, 1–29. (d) Juzeniene, A.; Peng, Q.; Moan, J. *Photochem. Photobiol. Sci.* **2007**, *6*, 1234–1245.

(3) (a) Che, C. M.; Yip, H. K.; Li, D.; Peng, S. M.; Lee, G. H.; Wang, Y. M.; Liu, S. T. *J. Chem. Soc., Chem. Commun.* **1991**, *161*, 5–1617. (b) Yam, V. W. W.; Fung, W. K. M.; Cheung, K. K. *Chem. Commun.* **1997**, *96*, 3–964. (c) Yam, V. W. W.; Lo, K. K. W. *Comments Inorg. Chem.* **1997**, *19*, 209–229. (d) Hettiarachchi, S. R.; Schaefer, B. K.; Yson, R. L.; Staples, R. J.; Herbst-irmer, R.; Patterson, H. H. *Inorg. Chem.* **2007**, *46*, 6997–7004. (e) Crespo, O.; Gimeno, M. C.; Laguna, A.; Larraz, C.; Villacampa, M. D. *Chem.−Eur. J.* **2007**, *13*, 235–246. (f) Green, A. R.; Presta, A.; Gasyna, Z.; Stillman, M. J. *Inorg. Chem.* **1994**, *33*, 4159–4168.

(4) (a) Cattaneo, M.; Fagalde, F.; Katz, N. E.; Borsarelli, C. D.; Parella, T. *Eur. J. Inorg. Chem.* **2007**, *34*, 5323–5332. (b) Kennedy, F.; Shavaleev, N. M.; Koullourou, T.; Bell, Z. R.; Jeffery, J. C.; Faulkner, S.; Ward, M. D. *Dalton Trans.* **2007**, 1492–1499.

(5) (a) Chi, Y.; Chou, P. T. *Chem. Soc. Rev.* **2007**, *36*, 1421–1431. (b) Anastasova, S.; Kapturkiewicz, A.; Nowacki, J. *Inorg. Chem. Commun.* **2005**, 1177–1180.

(6) (a) Marin, V.; Holder, E.; Hoogenboom, R.; Schubert, U. S. *Chem. Soc. Rev.* **2007**, *36*, 618–635. (b) Winter, A.; Ulbricht, C.; Holder, E.; Risch, N.; Schubert, U. S. *Aust. J. Chem.* **2006**, *59*, 773–782.

(7) (a) Lo, K. K. W.; Li, C. K.; Lau, K. W.; Zhu, N. Y. *Dalton Trans.* **2003**, 4682–4689. (b) Rourke, J.; Batsanov, A. S.; Howard, J. A. K.; Marder, T. B. *Chem. Commun.* **2001**, 2626–2627.

10.1021/ic801840g CCC: $40.75
Published on Web 03/04/2009

because their orbital energies are better matched and there will be greater delocalization of the spin electron density toward bridging atoms.[9] They can also work as reducing agents in in situ redox reaction under solvothermal conditions.[10] To obtain low-energy luminescence, we chose the ligands containing sulfur and a conjugated system to coordinate with coin metals; these ligands themselves can emit relatively low energy emission.[10a,11] By applying the appropriate bridging ligand, we have obtained a series of one-dimensional (1D), two-dimensional (2D), and three-dimensional (3D) complexes possessing interesting structural motifs and significant properties. For example, we previously reported a cuprous complex with 752 nm emission, where its unusually low energy emission or long emission wavelength was observed. Here we report two cuprous organosulfur complexes, $Cu_6(btt)_6$ (**1**) and $Cu_4(btt)_4$ (**2**), and an argentous complex $Ag_6(bmt)_6 \cdot 6THF$ (**3**) (Hbtt = 2-benzothiazolethiol, Hbmt = 2-benzimidazolethiol, and THF = tetrahydrofuran). Complex **1** exhibits NIR luminescence, which is very scarce in transition-metal complexes, while complexes **2** and **3** give red emissions at ambient atmosphere.

Experimental Section

Materials and Analyses. All chemicals were used as received without further purification. Fluorescent spectra were measured on an Edinburgh Instruments model FL920 analyzer. Thermal gravimetric (TG) analyses were performed with a heating rate of 15 °C·min^{-1} using a NETZSCH STA 449C simultaneous TG−differential scanning calorimetry instrument. Powder X-ray diffraction (XRD) patterns were collected on an X'Pert-Pro diffractometer using Cu Kα radiation (λ = 1.5406 Å) in the 2θ range of 5−85°. The generator voltage is 45 kV, and the tube current is 40 mA. Elemental analyses were carried out on an Elementar Vario EL III microanalyzer.

Computational Details. All theoretical calculations were performed by using the *GAUSSIAN03* program. The ground-state equilibrium geometries of complexes **1** and **2** were fully optimized using the hybrid functional B3P86 and the LANL2DZ ECP basis set with S_6 and S_4 symmetries, respectively.

Preparation of $Cu_6(btt)_6$ (1). The red crystals of complex **1** were prepared by solvothermal methods. $CuCl_2 \cdot 2H_2O$ (34 mg, 0.2 mmol) and 2,2′-dithiobis(benzothiazole) (dbt; 50 mg, 0.15 mmol) were added to a MeOH/MeCN solution (1:1, 7 mL) in a Teflon-lined stainless steel reactor. The mixture was heated at 90 °C for 3 days and then cooled to room temperature in 16 h. The crystals of **1** were collected and washed with MeCN and MeOH. Yield: 73.9% (34 mg) based on Cu. Anal. Calcd for $C_{42}H_{24}Cu_6N_6S_{12}$: H, 1.75; C, 36.59; N, 6.10. Found: H, 1.72; C, 36.65; N, 6.03.

Preparation of $Cu_4(btt)_4$ (2). Route 1. The same method as that of **1** was applied, but the reaction system was cooled to room temperature in 8 h. The crystals of **2** were collected and washed with MeCN and MeOH. Yield: 60.9% (28 mg) based on Cu. **Route 2.** $CuCl_2 \cdot 2H_2O$ (34 mg, 0.2 mmol) and 2-benzothiazolethiol (Hbtt; 33 mg, 0.2 mmol) were added to a MeOH solution in a Teflon-lined stainless steel reactor. The mixture was heated at 90 °C for 3 days and then cooled to room temperature in 4 h. The powder product of **2** was collected and washed with MeCN and MeOH. Yield: 19.6% (9 mg) based on Cu. Anal. Calcd for $C_{28}H_{16}Cu_4N_4S_8$: H, 1.75; C, 36.59; N, 6.10. Found: H, 1.80; C, 36.71; N, 6.16.

Preparation of $Ag_6(bmt)_6 \cdot 6THF$ (3). $AgNO_3$ (34 mg, 0.2 mmol), 2-benzimidazolethiol (Hbmt; 30 mg, 0.2 mmol), and MeONa (11 mg, 0.2 mmol) were added to 30 mL of tetrahydrofuran (THF) in sequence to give a light-yellow suspension. After stirring for 6 h, the mixture was filtered out, and the filtrate was allowed to evaporate at ambient atmosphere. Yellow crystals were isolated 5 days later. Yield: 56.8% (37.5 mg) based on Ag. Anal. Calcd for $C_{66}H_{84}Ag_6N_{12}O_6S_6$: H, 4.27; C, 40.02; N, 8.48. Found: H, 3.98; C, 39.26; N, 8.83.

Crystal Structural Determination. Intensity data for complexes **1**−**3** were measured on Rigaku Saturn 70 CCD and Rigaku Mercury CCD diffractometers, respectively, with graphite-monochromated Mo Kα radiation (λ = 0.710 73 Å) at 293 K. Empirical absorption corrections were applied using the *SADABS* program for the Siemens area detector. The structures were solved by direct methods, and all calculations were performed using the *SHELXL-97* program. The coordinate of metal atoms was obtained from the E map. The successive difference Fourier syntheses gave all of the coordinates of the non-hydrogen atoms. All non-hydrogen atoms were refined anisotropically. All hydrogen atoms were added in the riding model and refined isotropically with C−H = 0.96 Å. A summary of the crystallographic data of complexes **1**−**3** is listed in Table 1, and their selected bond lengths and angles are listed in Tables 2−4, respectively.

Results and Discussion

Single-crystal analysis has revealed that the hexanuclear cluster **1** has six Cu^I centers bridged by the btt ligands and figures as a distorted octahedron, as shown in Figure 1. Each Cu^I is bonded by two sulfur atoms and one nitrogen atom from three btt molecules to form a trigonal geometry. Each

(8) (a) Nastasi, F.; Puntoriero, F.; Palmeri, N.; Cavallaro, S.; Campagna, S.; Lanza, S. *Chem. Commun.* **2007**, 4740–4742. (b) Yam, V. W. W.; Chan, K. H. Y.; Wong, K. M. C.; Chu, B. W. K. *Angew. Chem., Int. Ed.* **2006**, *45*, 6169–6173. (c) Yam, V. W. W.; Cheng, E. C. C.; Cheung, K. K. *Angew. Chem., Int. Ed.* **1999**, *38*, 197–199. (d) Fernández, E. J.; Laguna, A.; López-de-Luzuriaga, J. M.; Monge, M.; Montiel, M.; Olmos, M. E.; Rodríguez-Castillo, M. *Organometallics* **2006**, *25*, 3639–3646.

(9) (a) Cheng, J. K.; Yao, Y. G.; Zhang, J.; Li, Z. J.; Cai, Z. W.; Zhang, X. Y.; Chen, Z. N.; Chen, Y. B.; Kang, Y.; Qin, Y. Y.; Wen, Y. H. *J. Am. Chem. Soc.* **2004**, *126*, 7796. (b) Kimblin, C.; Bridgewater, B. M.; Churchill, D. G.; Hascall, T.; Parkin, G. *Inorg. Chem.* **2000**, *39*, 4240. (c) Perruchas, S.; Boubekeu, K. *Dalton Trans.* **2004**, 2394. (d) Bu, X. H.; Hou, W. F.; Du, M.; Chen, W.; Zhang, R. H. *Cryst. Growth Des.* **2002**, *2*, 303–307. (e) Brooks, N. R.; Blake, A. J.; Champness, N. R.; Cunningham, J. W.; Hubberstey, P.; Schroder, M. *Cryst. Growth Des.* **2001**, *1*, 395. (f) del Rio, I.; Terroba, R.; Cerrada, E.; Hursthouse, M. B.; Laguna, M.; Light, M. E.; Ruiz, A. *Eur. J. Inorg. Chem.* **2001**, 2013.

(10) (a) Han, L.; Hong, M. C.; Wang, R. H.; Wu, B. L.; Xu, Y.; Lou, B. Y.; Lin, Z. Z. *Chem. Commun.* **2004**, 2578–2579. (b) Du, M.; Zou, R. Q.; Zhong, R. Q.; Xu, Q. *Inorg. Chem. Commun.* **2007**, *10*, 1437–1439.

(11) (a) Hong, M. C.; Su, W. P.; Cao, R.; Zhang, W. J.; Lu, J. X. *Inorg. Chem.* **1999**, *38*, 600. (b) Su, W. P.; Hong, M. C.; Weng, J. B.; Cao, R.; Lu, S. F. *Angew. Chem., Int. Ed.* **2000**, *39*, 2911. (c) Zhao, Y. J.; Hong, M. C.; Liang, Y. C.; Cao, R.; Li, W. J.; Weng, J. B.; Lu, S. F. *Chem. Commun.* **2001**, 1020. (d) Su, W. P.; Hong, M. C.; Weng, J. B.; Liang, Y. C.; Zhao, Y. J.; Cao, R.; Zhou, Z. Y.; Chan, A. S. C. *Inorg. Chim. Acta* **2002**, *331*, 8. (e) Su, W. P.; Cao, R.; Hong, M. C.; Wong, W. T.; Lu, J. X. *Inorg. Chem. Commun.* **1999**, *2*, 241. (f) Han, L.; Wu, B. L.; Xu, Y. Q.; Wu, M. Y.; Gong, Y. Q.; Lou, B. Y.; Chen, B. Q.; Hong, M. C. *Inorg. Chim. Acta* **2005**, *358*, 2005–2013. (g) Han, L.; Xu, Y. Q.; Wu, M. Y.; Gong, Y. Q.; Wu, B. L.; Hong, M. C. *Inorg. Chem. Commun.* **2005**, *8*, 529–532. (h) Han, L.; Wang, R. H.; Yuan, D. Q.; Wu, B. L.; Lou, B. Y.; Hong, M. C. J. *Mol. Chem.* **2005**, *737*, 55–59.

(12) (a) Xie, H. Y.; Kinoshita, I.; Karasawa, T.; Kimura, K.; Nishioka, T.; Akai, I.; Kanemoto, K. *J. Phys. Chem. B* **2005**, *109*, 9339–9345. (b) Bai, Y.; He, G. J.; Zhao, Y. G.; Duan, C. Y.; Dang, D. B.; Meng, Q. J. *Chem. Commun.* **2006**, 1530–1532.

Table 1. Crystallographic Data for Complexes **1**−**3**

	1	**2**	**3**
empirical formula	$C_{42}H_{24}Cu_6N_6S_{12}$	$C_{28}H_{16}Cu_4N_4S_8$	$C_{66}H_{84}Ag_6N_{12}O_6S_6$
fw	1378.63	919.09	1974.98
cryst color	red	yellow	yellow
cryst syst, space group	triclinic, $P\bar{1}$	tetragonal, $I\bar{4}$	hexagonal, $R\bar{3}m$
unit cell dimens	7.686(5) Å, 113.770(6)° 13.317(8) Å, 101.154(6)° 13.849(8) Å, 103.006(3)°	10.829(5) Å, 90° 10.829(5) Å, 90° 13.469(7) Å, 90°	16.7385(7) Å, 90° 16.7385(7) Å, 90° 23.8014(11) Å, 120°
volume	1198.1(13) Å^3	1579.5(13) Å^3	5775.2(4) Å^3
Z, calcd density	1, 1.911 Mg/m^3	2, 1.933 Mg/m^3	3, 1.709 Mg/m^3
abs coeff	3.178 mm^{-1}	3.215 mm^{-1}	1.714 mm^{-1}
$F(000)$	684	912	2952
cryst size	0.08 × 0.06 × 0.02 mm^3	0.12 × 0.10 × 0.10 mm^3	0.38 × 0.30 × 0.25 mm^3
θ range for data collection	2.82−27.47°	2.41−27.46°	3.29−27.50°
limiting indices	$-9 \le h \le 9$, $-17 \le k \le 17$, $-12 \le l \le 17$	$-11 \le h \le 14$, $-14 \le k \le 13$, $-14 \le l \le 17$	$-14 \le h \le 21$, $-21 \le k \le 16$, $-30 \le l \le 30$
reflns collected/unique	9545/5404 [R(int) = 0.0535]	6174/1805 [R(int) = 0.0245]	14851/1631 [R(int) = 0.0211]
completeness to θ	98.8% (θ = 27.47)	99.8% (θ = 27.46)	99.7% (θ = 27.50)
abs corrn	semiempirical from equivalents	semiempirical from equivalents	semiempirical from equivalents
max and min transmn	0.9392 and 0.7851	0.7393 and 0.6990	0.6739 and 0.5620
refinement method	full-matrix least squares on F^2	full-matrix least squares on F^2	full-matrix least squares on F^2
data/restraints/param	5404/0/298	1805/0/101	1631/0/125
GOF on F^2	1.038	1.029	1.021
final R indices [$I > 2\sigma(I)$]	R1 = 0.0616, wR2 = 0.0886	R1 = 0.0226, wR2 = 0.0480	R1 = 0.0532, wR2 = 0.1383
largest diff peak and hole	0.415 and −0.473 e A^{-3}	0.185 and −0.162 e A^{-3}	1.109 and −0.914 e A^{-3}

Table 2. Selected Bond Lengths (Å) and Angles (deg) for **1**[a]

Cu(1)−N(1)	2.016(4)	Cu(2)−Cu(3)	3.031(2)
Cu(1)−S(5)	2.245(2)	Cu(3)−N(3)#1	2.011(5)
Cu(1)−S(3)	2.2554(19)	Cu(3)−S(1)#1	2.2454(19)
Cu(1)−Cu(2)	3.0014(16)	Cu(3)−S(3)	2.253(2)
Cu(2)−N(2)	2.014(4)	S(1)−Cu(3)#1	2.245(2)
Cu(2)−S(1)	2.2449(18)	S(5)−Cu(2)#1	2.248(2)
Cu(2)−S(5)#1	2.248(2)	N(3)−Cu(3)#1	2.011(5)
N(1)−Cu(1)−S(5)	118.89(14)	S(5)#1−Cu(2)−Cu(1)	134.45(6)
N(1)−Cu(1)−S(3)	117.91(14)	N(2)−Cu(2)−Cu(3)	79.92(13)
S(5)−Cu(1)−S(3)	117.61(8)	S(1)−Cu(2)−Cu(3)	135.08(6)
N(1)−Cu(1)−Cu(2)	80.33(15)	S(5)#1−Cu(2)−Cu(3)	79.76(5)
S(5)−Cu(1)−Cu(2)	132.29(6)	Cu(1)−Cu(2)−Cu(3)	61.86(4)
S(3)−Cu(1)−Cu(2)	80.46(6)	N(3)#1−Cu(3)−S(1)#1	116.36(15)
N(2)−Cu(2)−S(1)	119.02(13)	N(3)#1−Cu(3)−S(3)	120.87(15)
N(2)−Cu(2)−S(5)#1	117.09(14)	S(1)#1−Cu(3)−S(3)	117.70(7)
S(1)−Cu(2)−S(5)#1	117.26(6)	N(3)#1−Cu(3)−Cu(2)	82.10(14)
N(2)−Cu(2)−Cu(1)	81.08(15)	S(1)#1−Cu(3)−Cu(2)	131.49(5)
S(1)−Cu(2)−Cu(1)	80.26(6)	S(3)−Cu(3)−Cu(2)	79.83(5)

[a] Symmetry transformations used to generate equivalent atoms: $-x + 1$, $-y + 1$, $-z$.

Table 3. Selected Bond Lengths (Å) and Angles (deg) for **2**[a]

Cu(1)−N(1)#1	2.002(3)	Cu(1)−Cu(1)#3	2.6620(11)
Cu(1)−S(1)#2	2.2453(12)	Cu(1)−Cu(1)#1	3.0505(16)
Cu(1)−S(1)	2.3027(14)		
N(1)#1−Cu(1)−S(1)#2	119.00(9)	S(1)−Cu(1)−Cu(1)#2	120.12(3)
N(1)#1−Cu(1)−S(1)	112.72(9)	Cu(1)#3−Cu(1)−Cu(1)#2	69.92(2)
S(1)#2−Cu(1)−S(1)	128.10(3)	N(1)#1−Cu(1)−Cu(1)#1	79.95(8)
N(1)#1−Cu(1)−Cu(1)#3	134.16(8)	S(1)#2−Cu(1)−Cu(1)#1	107.83(3)
S(1)#2−Cu(1)−Cu(1)#3	86.06(5)	S(1)−Cu(1)−Cu(1)#1	76.41(3)
S(1)−Cu(1)−Cu(1)#3	53.18(3)	Cu(1)#3−Cu(1)−Cu(1)#1	55.041(12)
N(1)#1−Cu(1)−Cu(1)#2	92.66(8)	Cu(1)#2−Cu(1)−Cu(1)#1	55.040(12)
S(1)#2−Cu(1)−Cu(1)#2	55.18(3)		

[a] Symmetry transformations used to generate equivalent atoms: #1, $-x + 2$, $-y + 2$, z; #2, $-y + 2$, x, $-z + 1$; #3, y, $-x + 2$, $-z + 1$.

btt molecule works as a μ_3-bridging ligand to link three different Cu^I ions (the nitrogen atom to one Cu^I ion and the axial μ_2-sulfur to two Cu^I ions), defining a face of an octahedron and shortening the distances between Cu^I ions. The Cu···Cu separations lie in the range of 3.001−3.100 Å, close to the sum of the van der Waals radii of two Cu^I atoms (2.80 Å),[12] illuminating the possible existence of

Table 4. Selected Bond Lengths (Å) and Angles (deg) for **3**[a]

Ag(1)−N(1)#1	2.221(5)	Ag(1)−Ag(1)#4	3.2386(8)
Ag(1)−S(1)	2.4853(12)	Ag(1)−Ag(1)#1	3.2386(8)
Ag(1)−S(1)#2	2.4853(12)	S(1)−Ag(1)#3	2.4853(12)
Ag(1)−Ag(1)#3	3.1494(9)	N(1)−Ag(1)#4	2.221(5)
Ag(1)−Ag(1)#2	3.1494(9)		
N(1)#1−Ag(1)−S(1)	113.83(5)	S(1)−Ag(1)−Ag(1)#4	80.96(3)
N(1)#1−Ag(1)−S(1)#2	113.83(5)	S(1)#2−Ag(1)−Ag(1)#4	134.88(3)
S(1)−Ag(1)−S(1)#2	125.04(7)	Ag(1)#3−Ag(1)−Ag(1)#4	60.906(9)
N(1)#1−Ag(1)−Ag(1)#3	136.76(9)	Ag(1)#2−Ag(1)−Ag(1)#4	90.0
S(1)−Ag(1)−Ag(1)#3	50.68(2)	N(1)#1−Ag(1)−Ag(1)#1	77.80(11)
S(1)#2−Ag(1)−Ag(1)#3	104.69(3)	S(1)−Ag(1)−Ag(1)#1	134.88(3)
N(1)#1−Ag(1)−Ag(1)#2	136.76(9)	S(1)#2−Ag(1)−Ag(1)#1	80.96(3)
S(1)−Ag(1)−Ag(1)#2	104.69(3)	Ag(1)#3−Ag(1)−Ag(1)#1	90.0
S(1)#2−Ag(1)−Ag(1)#2	50.68(2)	Ag(1)#2−Ag(1)−Ag(1)#1	60.906(9)
Ag(1)#3−Ag(1)−Ag(1)#2	60.0	Ag(1)#4−Ag(1)−Ag(1)#1	58.186(19)
N(1)#1−Ag(1)−Ag(1)#4	77.80(11)		

[a] Symmetry transformations used to generate equivalent atoms: #1, $y-1/3$, $-x + y + 1/3$, $-z + 1/3$; #2, $-x + y$, $-x + 1$, z; #3, $-y + 1$, $x - y + 1$, z; #4, $x - y + 2/3$, $x + 1/3$, $-z + 1/3$.

Cu···Cu interactions (Figure 3). The molecules expand to a 2D network in the bc plane via $\pi-\pi$ interactions with a plane-to-plane distance of 3.5027 Å (Figure 2a).

It is interesting that the Cu^I ions of complex **2** have coordination environments similar to those of complex **1**, but the whole molecule of **2** with a tetranuclear metal core appears much different. Two distorted hexagons (Cu_3S_3) are formed in **1** that are related by nitrogen-donor atoms and Cu−Cu short distances. However, in complex **2**, no such hexagon appears. The structure of **1** is much more open compared with that of **2**. There are two kinds of Cu···Cu separations in the structure of **2**: 2.662 and 3.051 Å, shorter than or close to the sum of the van der Waals radii of two Cu^I atoms (2.80 Å). Therefore, metal−metal bonds and weak metal···metal interactions are both found. No $\pi-\pi$ interactions are found in the structure of complex **2** (Figure 2b).

The molecule structure of complex **3** seems similar to that of complex **1**, where the hexanuclear cluster has six Ag^I centers bridged by bmt ligands (Figure 3). There are two kinds of Ag−Ag separations of 3.149 and 3.238 Å in **3**, which are shorter than the sum of the van der Waals radii of

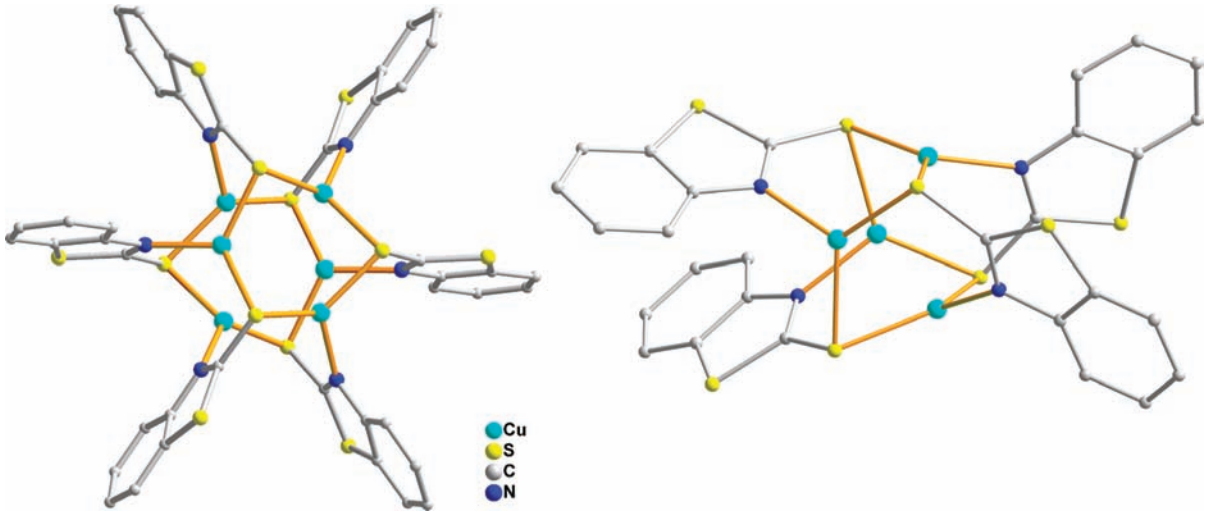

Figure 1. Coordination environments of Cu^{I} ions in **1** (left) and **2** (right). **3** is similar to **1**.

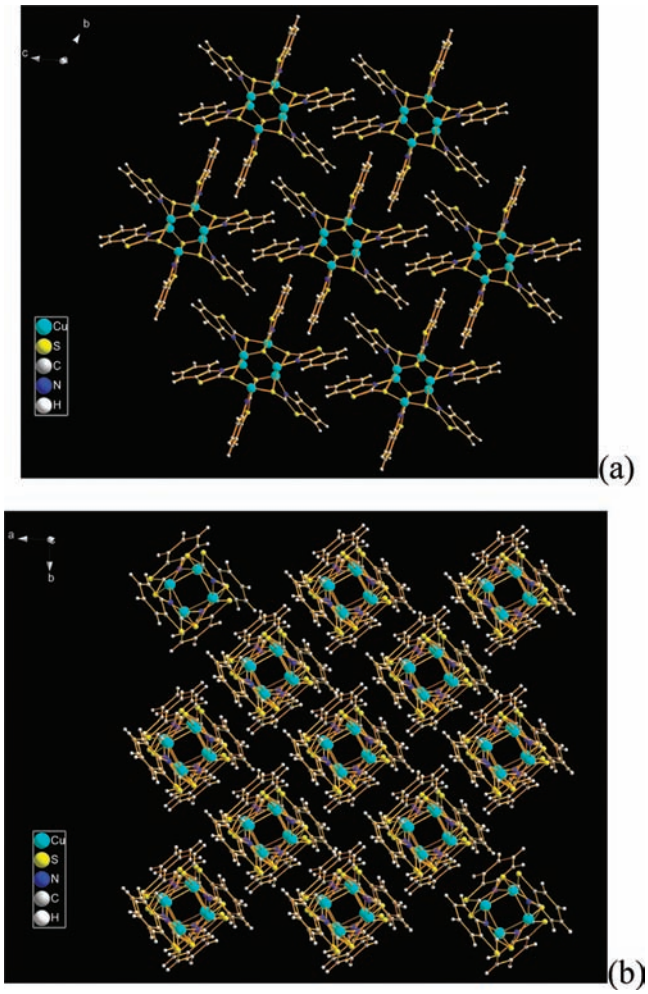

Figure 2. Packing structures of complexes **1** (a) and **2** (b).

two Ag^{I} atoms (3.40 Å),[13] illuminating the existence of Ag−Ag bonds. The solvent molecules, THF, lie between the clusters and can easily be moved away. Washed with ether, the freshly prepared light-yellow crystals **3** immediately turn pale. The pale sample can return to light yellow when it is wetted by a small amount of THF, implying that **3** here may act as a porous material with selective absorption.

The solvothermal reaction of Cu^{II} salt with dbt produced very fine red crystals of **1** or light-yellow crystals of **2**, where their original dbt molecules in both cases were broken up as Hbtt during heating. It was found that the cooling rate of the above reaction system had a significant influence on the production of **1** and **2**. If the reaction system was cooled to room temperature in 16 h, the red crystalline **1** with hexanuclear metal cores was obtained, while if it was cooled to room temperature in 8 h, the yellow crystalline product **2** with tetranuclear cores formed. When the cooling was finished in only 4 h, the yellow powder product was obtained, which proved via XRD to be complex **2**. The degree of crystallization for complex **2** is sensitive to the cooling rate, and such a phenomenon may be due to its lower growth rate of crystalline **2**. So, the slower cooling rate is in favor of crystallization of the above complex. The syntheses of complexes **1** and **2** seem interesting with several different routes, and their crystals can even grow together from the same substrates in an identical production flow. Obviously, this reaction resulted in an in situ redox process of copper, which was formerly proven by our group.[11a] Also, we performed the same experiment to conform to the mechanism

(13) Bondi, A. *J. Phys. Chem.* **1964**, *68*, 441.

(14) (a) Pope, S. J. A.; Coe, B. J.; Faulkner, S.; Laye, R. H. *Dalton Trans.* **2005**, 1482–1490. (b) Charmant, J. P. H.; Fornies, J.; Gomez, J.; Lalinde, E.; Merino, R. I.; Moreno, M. T.; Orpen, A. C. *Organometallics* **1999**, *18*, 3353–3358. (c) Adams, C. J.; Fey, N.; Weinstein, J. A. *Inorg. Chem.* **2006**, *45*, 6105–6107. (d) Guo, Z. G.; Cheng, C. H.; Fan, Z. Q.; He, W.; Yu, S. K.; Chang, Y. C.; Du, X. G.; Wang, X.; Du, G. T. *Chin. Phys. Lett.* **2008**, *25*, 715–718. (e) Yan, F.; Li, W. L.; Chu, B.; Li, T. L.; Su, W. M.; Su, Z. S.; Zhu, J. Z.; Yang, D. F.; Zhang, G.; Bi, D. F.; Han, L. L.; Cheng, C. H.; Yu, S. K.; Du, G. T.; Tsuboi, T. *Appl. Phys. Lett.* **2007**, *91*, 203512. (f) Yam, V. W. W.; Lo, K. K. W. *Chem. Soc. Rev.* **1999**, *28*, 323–334.

(15) Yin, G. Q.; Wei, Q. H.; Zhang, L. Y.; Chen, Z. N. *Organometallics* **2006**, *25*, 580–587.

(16) (a) Jess, I.; Taborsky, P.; Pospisil, J.; Naether, C. *Dalton Trans.* **2007**, 2263–2270. (b) Wang, H.; Li, M. X.; Shao, M.; He, X. *Polyhedron* **2007**, *26*, 5171–5176. (c) Yu, M. M.; Zhao, X. J.; Fu, W. F. *Chin. J. Struct. Chem.* **2007**, *26*, 1179–1183. (d) Dias, H. V. R.; Diyabalanage, H. V. K.; Eldabaja, M. G.; Elbjeirami, O.; Rawashdeh-Omary, M. A.; Omary, M. A. *J. Am. Chem. Soc.* **2005**, *127*, 7489–7501. (e) Iwamura, M.; Takeuchi, S.; Tahara, T. *J. Am. Chem. Soc.* **2007**, *129*, 5248–5256. (f) Yam, V. W. W.; Cheng, E. C. C. *Photochem. Photophys. Coord. Compd. II* **2007**, *281*, 269–309.

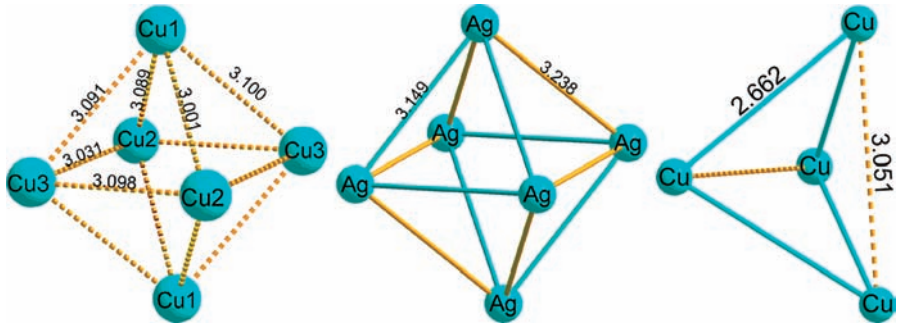

Figure 3. Distorted octahedral clusters formed by the hexanuclear cores in complexes **1** (left) and **3** (middle) and the distorted tetrahedron of the tetranuclear core in complex **2** (right).

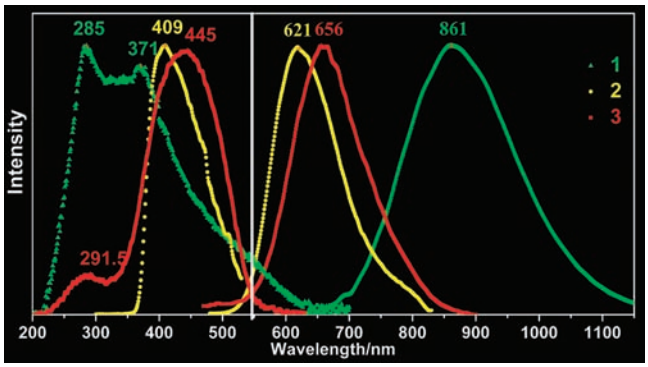

Figure 4. Solid excitation (left) and emission (right) spectra of complexes **1**−**3** at room temperature.

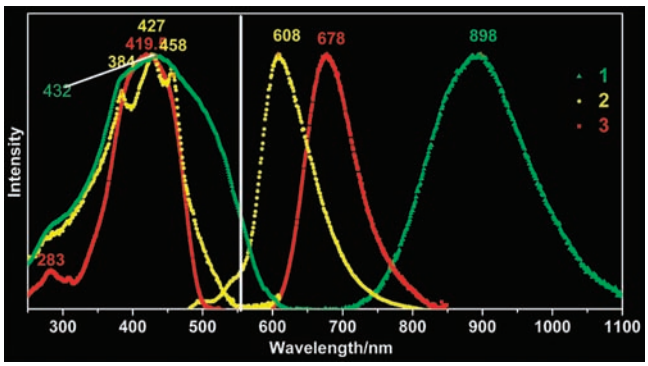

Figure 5. Solid excitation (left) and emission (right) spectra of complexes **1**−**3** at 77 K.

by the addition of a Ba^{2+} buffer solution into the acidic reaction filtrate, obtaining a small quantity of white precipitates. Notably, by the direct application of Hbtt and Cu^{I} salt instead of dbt and $CuCl_2$ in the preparations, complexes **1** and **2** can also be obtained but with lower yields.

The most fascinating characteristic of complex **1** is the unusual NIR emission, which is a very scarce phenomenon in the exploration of transition-metal complexes.[14] As shown in Figure 4, at room temperature, excitation of solid samples produces an intense NIR emission with a peak maximum at 861 nm. The solid-state lifetime at 298 K is in the range of microseconds (7.41 μs), revealing that the emission is phosphorescent, most likely associated with a spin-forbidden triplet parentage.[15] Hence, the relevant excited states have triplet spin multiplicity. Time-resolved emission measurements reveal that the NIR emission displays single-exponential decay kinetics with one decay time, suggesting the presence of one luminophor in a uniform environment.

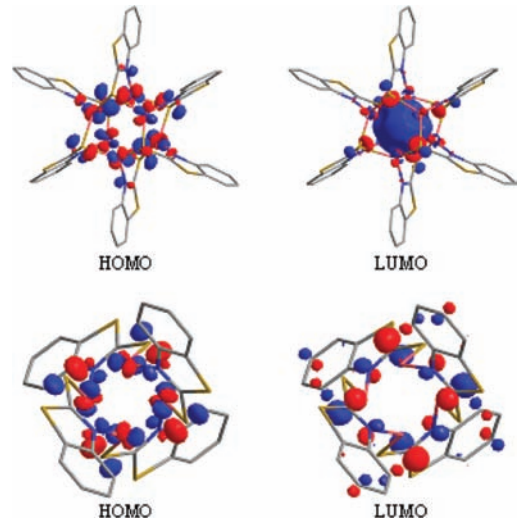

Figure 6. Electron-density distributions of the LUMO and HOMO frontier orbitals calculated for **1** (top) and **2** (bottom).

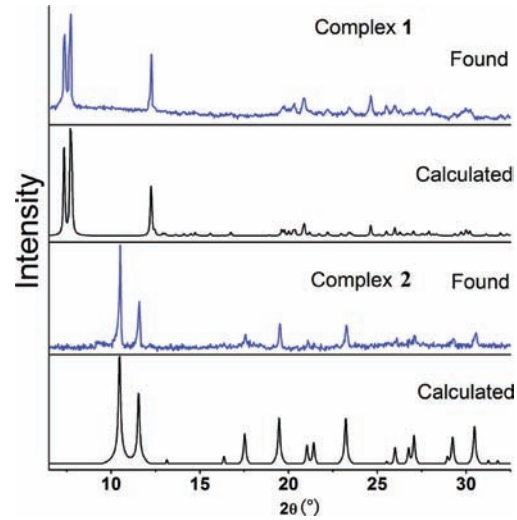

Figure 7. XRD patterns of complexes **1** and **2** (black, calculated sample; blue, as-synthesized sample).

It is noteworthy that this low-energy luminescence is unusual, representing the lowest energy emission or the longest emission wavelength, to our knowledge, in the luminescent d^{10} transition-metal complexes[16] to date, including the record of 752 nm that we reported.[11a]

With stronger metal−metal bonds and similar coordination modes compared to those of **1**, complex **2** produces a strong red emission at 621 nm, unexpectedly. The solid-state

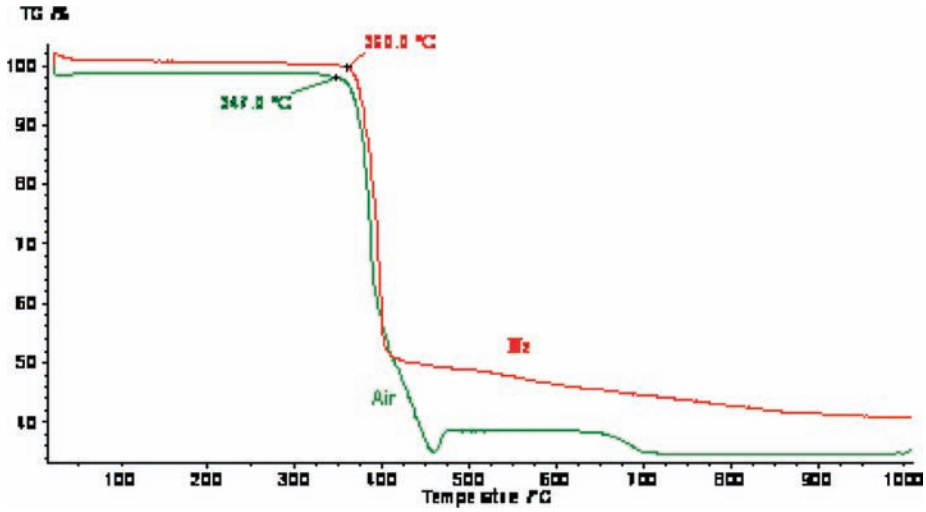

Figure 8. TG analysis for complex **1** under air and nitrogen atmospheres.

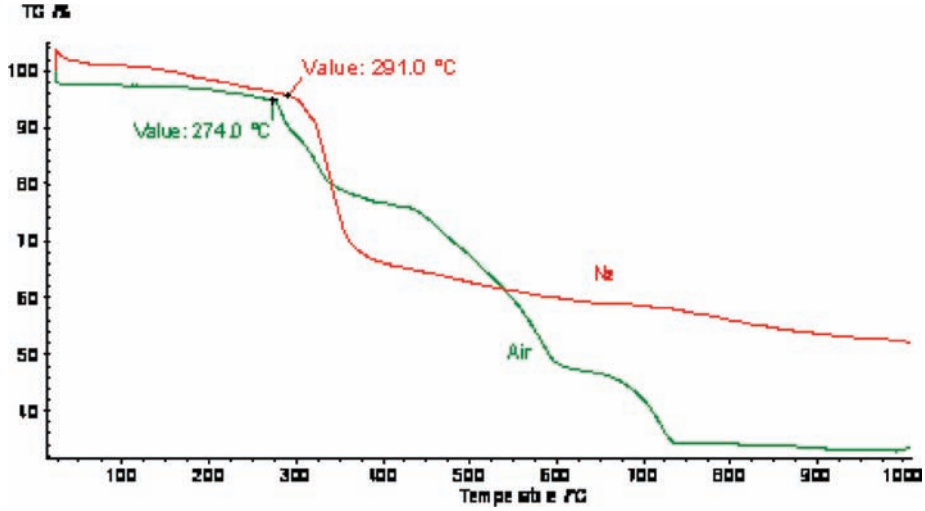

Figure 9. TG analysis for complex **2** under air and nitrogen atmospheres.

lifetime at 298 K is in the range of microseconds (6.62 μs), indicating that the emission is phosphorescent. Compared with the photoluminescent property of the free Hbtt ligand compound (λ_{max} = 654 nm), the emissions of complexes **1** and **2** seem widely red-shifted and narrowly blue-shifted, respectively. Complex **3** has red emission at 656 nm with a solid-state lifetime in the range of microseconds (0.197 μs), illuminating that the emission is phosphorescent. Similar to complex **1**, time-resolved emission measurements reveal that the emissions of complexes **2** and **3** also follow a single-exponential decay with one decay time. Compared with green luminescence at 526 nm of the free Hbmt, the emission of complex **3** demonstrates an obvious red shift. When frozen to 77 K, the emissions of complexes **1** and **3** shift to longer wavelengths of 898 and 678 nm, respectively. Oppositely, the emission of **2** blue-shifts with a peak emission at 608 nm (Figure 5).

As far as we know, most of the complexes with d_{Cu-Cu} less than or close to twice the van der Waals radius (1.4 Å) of Cu^I show low energy emission. Also, the longer wavelength luminescence derives from an excited state involving more than one metal center.[17] This means that the Cu−Cu distance plays a key role in the photoluminescence of cuprous complexes. With a longer metal−metal distance, complex **1** exhibits much lower energy emission compared to **2**, which is exceptional. To the best of our knowledge, the investigation about such lower energy emissions for complexes containing longer Cu−Cu distances (3.001−3.100 Å) remains relatively sparse. In a comparison with formerly reported results, of which the metal−metal distance plays a leading role for emission spectra, there are other crucial factors also working on the emission of complex **1**. All of the above could indicate that the excited states of complex **1** are very complicated and the simple sole excited-state model may not be accurate. In fact, several theories have been published to explain the electronic transition mechanism of the Cu^I complexes, but the photoluminescence of these complexes is not well understood so far.[18]

(17) Ford, P. C.; Cariati, E.; Bourassa, J. *Chem. Rev.* **1999**, *99*, 3625.
(18) (a) Coker, N. L.; Bauer, J. A. K.; Elder, R. C. *J. Am. Chem. Soc.* **2004**, *126*, 12–13. (b) Assefa, Z.; McBurnett, B.; Staples, R.; Fackler, J. P., Jr.; Assmann, B.; Angermaier, K.; Schmidbaur, H. *Inorg. Chem.* **1995**, *34*, 75–83.

Calculations were performed on **1** and **2** with their ground-state geometries adapted from the truncated X-ray data. The results indicate that the highest occupied molecular orbital (HOMO) of **1** is composed of d orbitals of Cu^I, while the lowest unoccupied molecular orbital (LUMO) mainly consists of s orbitals of Cu^I (Figure 6). Thus, if emission occurs from a state related to HOMO to LUMO excitation, in the excited state, the electron density has moved from Cu d orbitals to Cu s orbitals. Here we can assign the emission of **1** as a metal-centered triplet state modified by Cu−Cu interactions with Cu_6 clusters.[17] For complex **2**, the HOMO is also composed of d orbitals of Cu^I but the LUMO consists of d orbitals of Cu^I as well as π^* orbitals of benzothiazole (Figure 6). Thus, in the excited state, the electron density has moved from Cu d orbitals to π^* orbitals of benzothiazole. The emission may be assigned as a metal-to-ligand charge transfer. Similar to **1**, we assume that the red emission of **3** originates from a metal-centered triplet state modified by Ag−Ag interactions with Ag_6 clusters.

The synthesized products of **1** and **2** were characterized by powder XRD. As shown in Figure 7, the XRD patterns are well consistent with the results simulated from single-crystal data, illuminating the high purity of the as-synthesized samples. To investigate their thermal stabilities, TG analysis of **1** and **2** was carried out at the rate of 15 °C/min in both air and nitrogen atmospheres. Complex **1** exhibits high thermal stability in both air and nitrogen atmospheres. The sample starts to collapse at 347 and 360 °C, respectively. 65.07% mass loss is found in air at 458 °C, and the mass immediately increases, implying a certain chemical reaction at this temperature. The mass loss keeps 61.65% from 473 to 640 °C, and a further collapse takes place. A complete collapse happens at 700 °C, with a total mass loss of 65.19%. In nitrogen, the mass-loss process seems much easier with a one-step collapse (Figure 8). A rapid mass loss happens between 360 and 408 °C, and then the mass-loss rate reins in until 1000 °C. Complex **2** starts to collapse at 274 °C in air, and then a two-step collapse happens. Heating above 735 °C results in a complete collapse of **2** and is accompanied by a rapid mass change as the organic component burns off. However, in nitrogen, it begins to a very slowly collapse with heating above 291 °C, followed by a rapid collapse until 378 °C. Complex **2** exhibits a lower thermal stability compared to **1** because of their differences in molecular structure (Figure 9).

Conclusion

In summary, three polynuclear $d^{10}-d^{10}$ transition-metal complexes **1**−**3** were synthesized with organosulfur ligands through solvothermal redox reactions and ambient reaction in solution, respectively, producing NIR or red luminescence. The cooling rate in the solvothermal syntheses resulted in distinct results for the crystal products **1** and **2**. This may introduce a new strategy in the design of functional materials. Their low cost, efficient synthetic routes, excellent luminescent properties, and thermal stabilities provide a practical origin of photoluminescent materials. Further exploration in this field is in progress in our group.

Acknowledgment. We are thankful for financial support from the 973 Program (Grant 2006CB932900), National Nature Science Foundation of China (Grant 20571074), and Nature Science Foundation of Fujian Province (Grant 2007J0172).

Supporting Information Available: Computational details, table of excitation energies and oscillator strengths for **1** and **2**, and crystallographic data in CIF format. This material is available free of charge via the Internet at http://pubs.acs.org.

IC801840G